

Identification of Primary Crystals in ZrTiCuNiBe Metallic Bulk Glasses

N. Wanderka¹, Q. Wei², I. Sieber¹, U. Czubayko¹ and M.-P. Macht¹

¹ Hahn-Meitner-Institut Berlin GmbH, Glienicker Str. 100, DE-14109 Berlin, Germany

² Max-Planck-Institut für Mikrostrukturphysik Halle, Weinbergweg 2, DE-06120 Halle, Germany

Keywords: Bulk Metallic Glasses, Primary Crystals, Field Ion Microscopy with Atom Probe, Transmission Electron Microscopy

Abstract. ZrTiCuNiBe metallic glasses which can be produced by comparably slow solidification of the liquid melt contain small fractions of primary crystals. These primary crystals were investigated by TEM, TEM/- and SEM/EDX, and FIM/AP. The chemical composition of the crystals was found to be ZrBe₂ with small Ti, Cu and Ni additions. The size, volume fraction and morphology of the primary crystals depend on the cooling rate. The tendency of crystal formation increases with higher Be contents. The crystallization behavior can be correlated to constitutional properties of the quasi-ternary ZrTi-CuNi-Be system.

Microdiffraction patterns obtained with a nearly parallel electron beam and a small spot size in connection with CBED and SAD methods were used to identify and characterize the crystal structure and its space group. By these techniques it was found that the crystals had an orthorhombic ordered structure with lattice parameters of $a = 0.37$ nm, $b = 0.66$ nm, $c = 0.63$ nm, and a space group Cmmm(65).

Introduction

During the production process of ZrTiCuNiBe bulk glasses [1] small fractions of primary crystals are formed [2,3]. The existence of these primary crystals diminishes the properties of the glass, e.g. its strength and corrosion behaviour. Unfortunately it is difficult to detect by standard X-ray diffraction (XRD) small fractions (< 1 %) of crystals in the glass. Therefore, to obtain information about the nature and origin of the primary crystals in the ZrTiCuNiBe bulk glasses the material was investigated by complementary high resolution analytical methods.

As has been reported previously [4] the primary crystals are rich in Be. Their composition is 64.5 Be - 31.6 Zr - 1.5 Ti - 1.4 Ni - 1.0 Cu (in at.%) which corresponds to ZrBe₂ with small additions of Ti, Ni and Cu. However, the structure of these crystals is not hexagonal, as would be anticipated from the binary ZrBe₂ phase. Instead, according to our transmission electron microscope (TEM) results, it has an orthorhombic structure. In the present work the structure of this phase is elucidated in more detail by microdiffraction technique [5], and the differences to the ZrBe₂ phase are demonstrated. Moreover, the morphology, size, structure and chemical composition of these crystals are studied. The results are discussed with respect to the constitutional behavior of the alloy.

Experimental Procedure

Two bulk glasses, Zr₄₁Ti₁₄Cu_{12.5}Ni₁₀Be_{22.5} (V1) and Zr_{46.8}Ti_{8.2}Cu_{7.5}Ni₁₀Be_{27.5} (V4) were produced by alloying the pure components by induction melting in a levitation device under purified Ar atmosphere and quenching by contact with a water cooled copper surface. Thus glassy ingots of

about 15 mm thickness and 20 mm diameter were obtained. This material was remelted in a fused silica crucible and die-cast into a copper mold, to obtain 60 mm long rods with diameters between 3 mm and 15 mm. This resulted in different average cooling rates, which were > 20 K/s for the rods of 5 mm in diameter and should be about one order of magnitude smaller for the 15 mm rods. However, it can be expected, that the cooling rate of the outer zones of the rods is considerably higher than the average rate due to the limited heat conduction in these alloys.

Microstructural analyses were performed by means of TEM. Energy dispersive analysis of X-ray emission (EDX) in TEM and SEM, and FIM/AP were used to analyze the chemical composition of the primary crystals and of the amorphous phase.

Discs with a diameter of 3 mm and a thickness of 0.3 mm, suitable for TEM, were thinned electrochemically at 263 K using a solution of 10% perchloric acid in ethanol and a potential of 30 V. For the investigation a Philips CM 30 electron microscope was used. The crystal structure and symmetry of the crystalline phase were deduced from microdiffraction patterns obtained with a nearly parallel electron beam and a small spot size in connection with convergent beam electron diffraction (CBED) and selected area electron diffraction (SAED) methods.

The crystal morphology was examined by optical microscopy, and by a SEM in a HITACHI S-4100 with field emission cathode. The composition of the crystals and amorphous matrix was determined by energy dispersive X-ray analysis with a Si-Q detector.

Small rods with a cross section of 0.2 mm x 0.2 mm and a length of 15 mm for FIM/AP were cut from the bulk material. They were electrolytically formed to sharp FIM tips in a solution of 15% perchloric acid in acetic acid at a voltage of 16-20 V DC at room temperature. Subsequently, the tips were polished using ion milling with 5 kV Ar^+ ions at liquid nitrogen temperature. In order to analyse the crystalline phase a special preparation technique for the FIM tips as described in [6] was also used. An energy-compensated time-of-flight atom probe VG FIM 100 was used in the present work. The atom probe analyses were performed at 70 K with a ratio of 20% between pulse voltage and permanently applied voltage.

3. Results and Discussion

3.1 Formation of primary crystals

The number, size and morphology of the primary crystals depend on the composition of the alloy and on the cooling rate. For high cooling rates > 20 K/s (≤ 5 mm rods) no primary crystals can be detected. In V1 rods of 12 mm diameter and ingots of 15 mm thickness only a small number of primary crystals can be observed. This material contains a number density between 10^8 and $10^{10}/\text{m}^3$ of Zr rich crystals with 10 to 20 μm size and dendritic morphology [4]. V4 rods up to 7 mm diameter contain similar number of crystals as in V1 rods with 12 mm diameter. These volume fractions of crystalline particles are too small to be detected by XRD.

Fig. 1 shows optical micrographs of the microstructure of V4 glass specimens produced under two different cooling conditions. In rods of 12 mm diameter a large number of crystals with „hollow prismatic“ shape up to a length of 100 μm and a width of 10 μm are observed (Fig. 1a). However, an outer shell of about 1 mm width at the surface of the rod is free from crystals, probably due to the much faster cooling rate in this zone. The crystal size increases towards the center of the rod. XRD of this material shows bragg peaks corresponding to the ZrBe_2 phase superimposed on the broad maxima of the amorphous matrix. Around the prismatic crystals denuded zones in the glassy matrix become visible by contrast variation in the SEM image. In a few cases in the denuded zones a second crystalline phase is visible which shows a fine structure on the micrometer scale. The composition of the „hollow prisms“ corresponds to ZrBe_2 with small additions of Ti, Ni, and Cu [4]. Therefore, the denuded zones are expected to be depleted of Be and enriched in all other components of the alloy. In fact, deviations of the concentration of Zr and Ni between crystals and their surrounding were observed by SEM/EDX. In some cases FIM/AP analysis indicated Be

depletion and enrichment of Ni and Ti near the crystals (see Table 1). However, the latter data show a large scatter which may be caused by inhomogeneities: although the amorphous state of the matrix

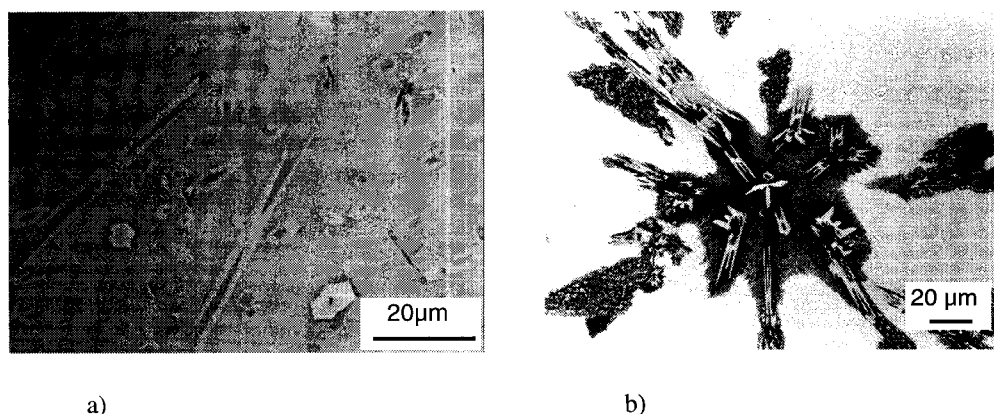


Fig. 1 Optical micrographs of the microstructure of the $\text{Zr}_{46.8}\text{Ti}_{8.2}\text{Cu}_{7.5}\text{Ni}_{10}\text{Be}_{27.5}$ (V4) alloy produced under two cooling rates a) > 20 K/s with „hollow prismatic“ crystals, and b) < 20 K/s with decorative „character“ crystals and dendritic structure around the „characters“.

around and inside the „hollow prism“ crystals could be verified by electron diffraction with TEM, the FIM/AP analysis might have been performed near such „hollow prism“ crystals around which the second crystalline phase was formed.

During slower solidification of the V4 melt (cooling rates < 20 K/s, Fig. 1b), e.g. by production of ingots of 15 mm thickness or of die-cast rods of > 12 mm diameter, the number of the primary crystals increases to values of $> 10^{12}/\text{m}^3$. The morphology of these crystals becomes more complicated. The „hollow prisms“, with cross sections like „nuts“ get several symmetrical protrusions, thus getting the shape of decorative „characters“ (see Fig. 1b).

Large (about $100\text{ }\mu\text{m}$) and small ($1 - 5\text{ }\mu\text{m}$) crystallites are arranged in a fashion which resembles self-organized, fractal structures. These objects are distributed rather inhomogeneously in the bulk. A crystalline dendritic structure around and between the large primary crystals is also visible in the optical and the SEM micrographs. Moreover, at the outer border of the „character“ like crystals denuded zones become visible again.

Table 1. Chemical composition of the amorphous matrix and the „hollow prism“ crystals from FIM/AP analysis and nominal composition of the $\text{Zr}_{46.8}\text{Ti}_{8.2}\text{Cu}_{7.5}\text{Ni}_{10}\text{Be}_{27.5}$ (V4) glass.

| Elem. | Amorph. No.1 | Amorph. No.2 | Amorph. No.3 | Amorph. No.4 | Amorph. No.5 | Nominal Comp. | "hol. prism" |
|-------|-----------------|-----------------|-----------------|-----------------|-----------------|------------------|-----------------|
| Be | 22.3 ± 3.5 | 17.2 ± 2.3 | 19.5 ± 2.1 | 30.8 ± 1.9 | 35.9 ± 3.1 | 27.5 | 64.5 ± 3.6 |
| Ti | 9.8 ± 2.5 | 11.3 ± 1.9 | 9.9 ± 1.5 | 11.7 ± 1.3 | 9.3 ± 1.9 | 8.3 | 1.5 ± 0.9 |
| Ni | 12.6 ± 2.8 | 11.9 ± 2.0 | 16.1 ± 1.9 | 8.0 ± 1.1 | 13 ± 2.2 | 10 | 1.4 ± 0.9 |
| Cu | 5.7 ± 2.0 | 8.4 ± 1.7 | 7.6 ± 1.4 | 5.9 ± 1.0 | 4.8 ± 1.4 | 7.5 | 1 ± 0.8 |
| Zr | 49.5 ± 4.2 | 51.5 ± 3.0 | 47 ± 2.6 | 44.2 ± 2.1 | 37 ± 3.1 | 46.8 | 31.6 ± 3.5 |

Results of SEM/EDX measurements of the composition (without Be) of the „character“ like crystals, of the fine dendritic structure and of the amorphous matrix far away from the crystalline zone are listed in Table 2 together with the nominal alloy composition and the FIM/AP results of the „hollow prisms“ (all without consideration of Be). Obviously, the composition of the „character“ like crystals is similar to that of the „hollow prisms“. Scanning-Auger analysis of the fine dendritic structure around the „character“ like crystals showed significant depletion of Be and enrichment of all other components of the alloy. Because of the limited spatial resolution of the SEM/EDX analysis only integral measurements of this structure are possible. Nevertheless, these crystalline areas show an enrichment of Ni (e.g. No. 1 in Table 2) or Cu (e.g. No. 2 in Table 2) and depletion of Zr leading to a composition close to that of the second crystalline phase which forms during very slow cooling (0.01 K/s) of the V1 - melt.

Table 2. Chemical composition (without Be) of the „character“ like crystals, of the different areas with fine dendritic structure and of the amorphous matrix far away from the crystalline zone measured by EDX/SEM together with the nominal alloy composition and „hollow prism“ measured by FIM/AP in the $\text{Zr}_{46.8}\text{Ti}_{8.2}\text{Cu}_{7.5}\text{Ni}_{10}\text{Be}_{27.5}$ (V4) glass.

| Element | „characters“ | „hol. prism“ | Nominal | Amorph. | dendritic phases, EDX/SEM | | |
|---------|----------------|----------------|---------|----------------|---------------------------|----------------|----------------|
| | EDX/SEM | FIM/AP | Compos. | EDX/SEM | No. 1 | No. 2 | No..3 |
| Zr | 87.3 ± 0.5 | 89.0 ± 3.5 | 64.5 | 62.3 ± 0.5 | 55.5 ± 0.4 | 57.8 ± 0.4 | 58.9 ± 0.4 |
| Ti | 4.7 ± 0.1 | 4.2 ± 0.9 | 11.4 | 12.9 ± 0.2 | 15.7 ± 0.2 | 10.9 ± 0.1 | 13.1 ± 0.3 |
| Ni | 2.5 ± 0.3 | 3.9 ± 0.9 | 13.8 | 14.4 ± 0.5 | 20.6 ± 0.4 | 13.1 ± 0.4 | 16.2 ± 0.5 |
| Cu | 4.7 ± 0.4 | 2.8 ± 0.8 | 10.3 | 10.4 ± 0.6 | 8.2 ± 0.5 | 18.2 ± 0.6 | 11.8 ± 0.6 |

The microstructure of these slowly cooled melts also shows local correlations between the crystalline phases forming successively during the solidification of the liquid. Obviously, during this process the crystallization of the preceeding phase induces the crystallization of the following one because of constitutional reasons. Furthermore, the crystallization always starts by formation of a phase which is closely related to ZrBe_2 , a prominent intermetallic equilibrium phase of the Zr-Be binary alloy which is closest to the composition of the V1 and V4 alloys. The larger tendency of V4 to form ZrBe_2 primary crystals may be explained by its higher Be content. Despite of this constitutional tendency to facilitate the formation of crystalline phases the sluggish atom transport in these systems [7,8] limits even at cooling rates < 20 K/s the decomposition of the melt and hence retards the crystallization considerably. The influence of the sluggish atom transport is probably also visible in the special morphology of the primary and secondary crystals as described above.

3.2 Structure and symmetry of the ordered orthorhombic phase.

The diffraction patterns of pure hexagonal ZrBe_2 and of the orthorhombic ZrBe_2 phases with additions of Ti, Cu and Ni are very similar although the unit cell of both structures is quite different. The lattice parameters of orthorhombic phase are: $a=0.37\text{nm}$, $b=0.66\text{nm}$ and $c=0.63\text{nm}$, and those of the hexagonal phase are: $a=0.38\text{nm}$ and $c=0.32\text{nm}$. Whereas the a parameter of both phases is practically identical the c parameter of the orthorhombic phase is twice that of the hexagonal. The additions of Ti, Cu and Ni are responsible for the expansion of the unit cell. A transformation from

a binary hexagonal phase to an orthorhombic structure by additions of a third component is well known [9-11].

The pattern of $[10\bar{1}1]$ and $[10\bar{1}2]$ zones of the hexagonal phase are equivalent to the $[201]$ and $[101]$ directions of the orthorhombic phase. The orthorhombic symmetry of this phase is confirmed by CBED (microdiffraction). The whole pattern symmetry of the $[001]$ zone axis is $2mm$ while the

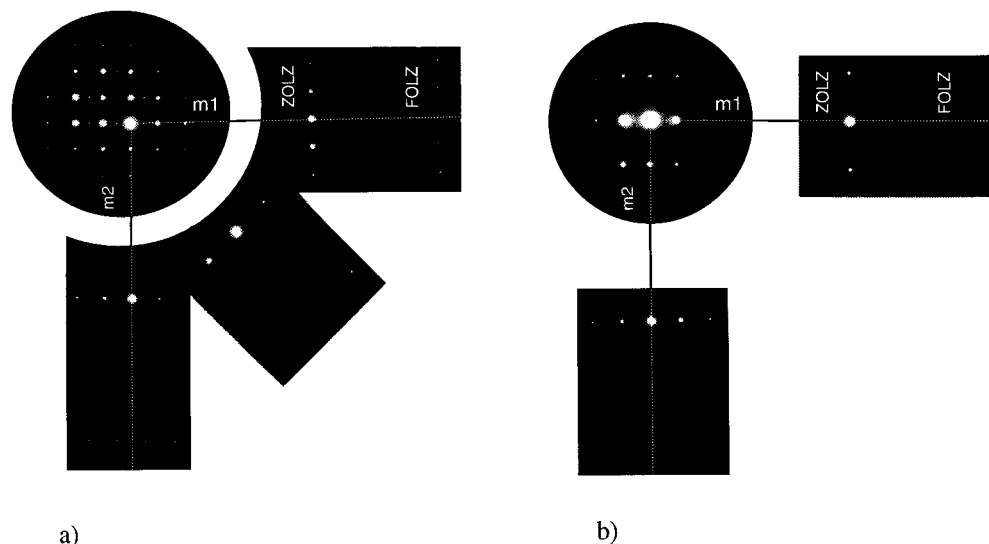


Fig. 2 Microdiffraction patterns of the „hollow prismatic“ crystals with orthorhombic structure: a) $[100]$ zone axis with $2mm$ symmetry in ZOLZ and $2mm$ symmetry in FOLZ; and b) $[010]$ zone axis, ZOLZ and whole patterns show $2mm$ symmetry. Both $[100]$ and $[010]$ FOLZ pattern can be obtained only by tilting the specimen along the mirrors $m1$ and $m2$.

whole pattern symmetry of the $[0001]$ zone axis of the hexagonal binary phase is $6mm$. Fig. 2a shows a zero-order laue zone (ZOLZ) pattern of $[100]$ zone axis, which has a $2mm$ symmetry. The diameter of the first-order laue zone (FOLZ) is quite large. Therefore the symmetry of FOLZ can be deduced only by tilting the sample along each of the symmetry elements present in the ZOLZ until reflections belonging to the FOLZ appear in the pattern. The FOLZ of $[100]$ has also a $2mm$ symmetry (see Fig. 2a). Therefore, there is a $2mm$ whole pattern symmetry in the $[100]$ zone axis. Such symmetries in both ZOLZ and whole patterns of $[100]$ zone axis uniquely implies a mmm point group symmetry by comparing with table 4 of [5]. There is no difference between the periodicities of ZOLZ- and FOLZ reflections. Furthermore, no shift between the reflection nets has been observed. The same analysis has been carried out in the $[010]$ zone axis (see Fig. 2b). Both ZOLZ and whole patterns show $2mm$ symmetry. There is also no difference between the periodicities of ZOLZ and FOLZ reflections but a shift between the reflection nets. The absence of periodicity differences between ZOLZ and FOLZ reflections implies that there are no gliding planes parallel to (100) , (010) and (001) . The shift of the ZOLZ and FOLZ reflection nets gives the information about the Bravais lattice. Therefore the structure must be an end-centered orthorhombic (A, B or C) lattice. The space group of this orthorhombic phase is identified as $Cmmm(65)$.

The result of the structure analysis indicates that the primary crystals in the $ZrTiCuNiBe$ alloys have an ordered structure composed of many differently sized atoms and comparatively large unit cell. Considerable transport as well as local rearrangement of atoms is necessary not only to provide for

the exact composition but also for the rather complicated, long range ordered crystal structure. Since diffusion in the alloys is sluggish, formation and growth of the primary crystals should be also slow even during slow cooling of the material from the melt, resulting in the excellent glass forming ability of these alloys.

Summary

Primary crystals which form during the production of ZrTiCuNiBe bulk glasses were investigated with respect to their structure, composition and morphology. It was found, that their composition is close to ZrBe₂, with small additions of Ti, Cu and Ni. They are of orthorhombic structure with Cmmm(65) symmetry.

The size, volume fraction and morphology of the primary crystals depend on the cooling rate. The tendency to form crystals depends on the alloy composition, it increases with higher Be content. The crystallization behavior was correlated to constitutional properties of the quasi ternary ZrTi-CuNi-Be system.

Acknowledgments

The authors would like to thank Dr. V. Naundorf for critical reading and discussions of the manuscript.

References

- [1] W. L. Johnson and Peker, Appl. Phys. Lett. 63 (1993) 2342
- [2] Q. Wei, Ph. D. thesis, University Potsdam, 1998
- [3] Q. Wei, N. Wanderka, P. Schubert-Bischoff, M.-P. Macht and S. Friedrich, to be published.
- [4] N. Wanderka, U. Czubyko, P. Schubert-Bischoff, M.-P. Macht, Mater. Sci. and Eng. A, in press
- [5] J. P. Morniroli and J.W. Steeds, Ultramicroscopy 45 (1992) 219
- [6] N. Wanderka, P. Schubert-Bischoff, M.-P. Macht and H. Wollenberger, Proceedengs of 11th European Congress on Electron Microscopy, 26th-30th August, Dublin, Vol. 1 (1996)
- [7] P. Fielitz, M.-P. Macht, V. Naundorf and G. Froberg, J. Non. Cryst. Sol., in press
- [8] A. Masuhr, R. Busch and W. L. Johnson, J. Non. Cryst. Sol. in press
- [9] D. Benerjee, Intermetallic Compounds: Vol. 2, Practice, edited by J. H. Westbrook and R. L. Fleischer 1994 John Wiley & Sons Ltd, p. 91
- [10] D. Benerjee, A. K. Gogia, T. K. Nandi and V. A. Joshi, Acta Met. 36 (1988) 871
- [11] B. Mozer, L. A. Bendersky, W.J. Boettinger and R. Grant Rowe, Scripta Met. 24, (1990) 2363